

# $G_0W_0$ for Molecules

Thesis by  
Patryk Kozłowski

In Partial Fulfillment of the Requirements for the  
Degree of  
Bachelor of Science in Chemistry

The Caltech logo, featuring the word "Caltech" in a bold, orange, sans-serif font.

CALIFORNIA INSTITUTE OF TECHNOLOGY  
Pasadena, California

2024  
Defended [Exact Date]

© 2024

Patryk Kozłowski  
ORCID: 0009-0000-6402-4261

All rights reserved

## ACKNOWLEDGEMENTS

[Add acknowledgements here. If you do not wish to add any to your thesis, you may simply add a blank titled Acknowledgements page.]

## ABSTRACT

[This abstract must provide a succinct and informative condensation of your work. Candidates are welcome to prepare a lengthier abstract for inclusion in the dissertation, and provide a shorter one in the CaltechTHESIS record.]

# TABLE OF CONTENTS

Acknowledgements . . . . .	iii
Abstract . . . . .	iv
Table of Contents . . . . .	v
List of Illustrations . . . . .	vi
List of Tables . . . . .	vii
Chapter I: Nomenclature . . . . .	1
Chapter II: Motivation . . . . .	2
Chapter III: Theoretical Background . . . . .	4
3.1 Mean Field Methods . . . . .	4
3.2 Many-body perturbation theory . . . . .	5
Chapter IV: $G_0W_0$ Procedure . . . . .	6
4.1 Iterative equation . . . . .	6
4.2 Correlation Self-Energy . . . . .	9
4.3 Random Phase Approximation . . . . .	9
Chapter V: Linearized $G_0W_0$ Density Matrix . . . . .	11
Chapter VI: This is the Sixth Chapter . . . . .	14
Chapter VII: This is the Seventh Chapter . . . . .	15
Chapter VIII: This is the Eighth Chapter . . . . .	16
Bibliography . . . . .	17
Appendix A: Questionnaire . . . . .	18
Appendix B: Consent Form . . . . .	19
Pocket Material: Map of Case Study Solar Systems	

## LIST OF ILLUSTRATIONS

<i>Number</i>	<i>Page</i>
2.1 Difference in the HOMO energy for the water molecule with different bases (cc-pVDZ, etc.) for $G_0W_0$ , and DFT, both starting from the PBE functional . . . . .	3
5.1 Natural occupations of the HOMO (State 1) and LUMO (State 2) of $H_2$ along the dissociation coordinate . . . . .	12
5.2 MO diagram of $H_2$ at the equilibrium bond distance. Notice that the HOMO is fully occupied with 2 electrons, while the LUMO is unoccupied. Figure from Bruneval [8] . . . . .	13

## LIST OF TABLES

*Number**Page*

# Chapter 1

## NOMENCLATURE

This uses the restricted Hartree-Fock formalism, meaning that two electrons with opposite spin occupy each spatial orbital.

Symbol	Description
$i, j, k, l$	Occupied orbital indices
$a, b, c, d$	Virtual orbital indices
$p, q, r, s$	General MO indices
$\mu, \nu, \lambda, \sigma$	AO indices
$(pq rs) = \int \int \psi_p^*(\mathbf{r}_1)\psi_q(\mathbf{r}_1)\frac{1}{r_{12}}\psi_r^*(\mathbf{r}_2)\psi_s(\mathbf{r}_2)d\mathbf{r}_1d\mathbf{r}_2$	Two-electron integrals
$(pq  rs) = (pq rs) - (ps rq)$	Antisymmetrized two-electron integrals

All calculations have been done using the PySCF package.<sup>1</sup> The code for this project can be found at [https://github.com/pkozlows/gw\\_senior\\_thesis/tree/master](https://github.com/pkozlows/gw_senior_thesis/tree/master).



## Chapter 2

### MOTIVATION

The formalism of many-body perturbation theory (MBPT) provides corrections to a mean-field description such as that given by Hartree-Fock or density functional theory (DFT). The former method does not treat electron correlation at all, and the latter one treats it in an average way. DFT is often used for systems of large size, as it is fairly accurate and computationally cheap. However, DFT's reliance on empirically based functionals in some cases gives rise to the notorious self-interaction error; because one is considering an electron in the average field of the electrons in the system, you can have an electron interacting with itself. In practice, this can potentially lead to a variety of issues, including the underestimation of surface stability (overestimation of surface energies) relevant in surface science studies.<sup>2</sup> To remedy this problem, normally one would fall back onto the wave function-based MBPT methods, such as coupled cluster theory (CC) and Moller-Plesset perturbation theory to 2nd order (MP2). However, their computational scaling is steep for larger systems, such as periodic ones.<sup>3</sup> Because of this issue, the perturbative methods often are not a better option than the field-standard DFT in predicting the properties of materials, as I have learned in a previous study.<sup>4</sup> Therefore, in the quantum chemistry community, there has been an interest in applying Green's function MBPT methods, with the  $GW$  approximation, to such systems, which has shown to give accurate corrections to, for example, band gaps, on top of a prior (DFT) mean-field calculation, at a cheap computational cost.<sup>5</sup> This is the motivation for my study of the  $G_0W_0$  method.

Figure 2.1 quantifies the potential of greens function methods, such as  $G_0W_0$ . As can be seen,  $G_0W_0$  lowers the orbital energy and, thus, captures more of the electronic correlation, as desired.

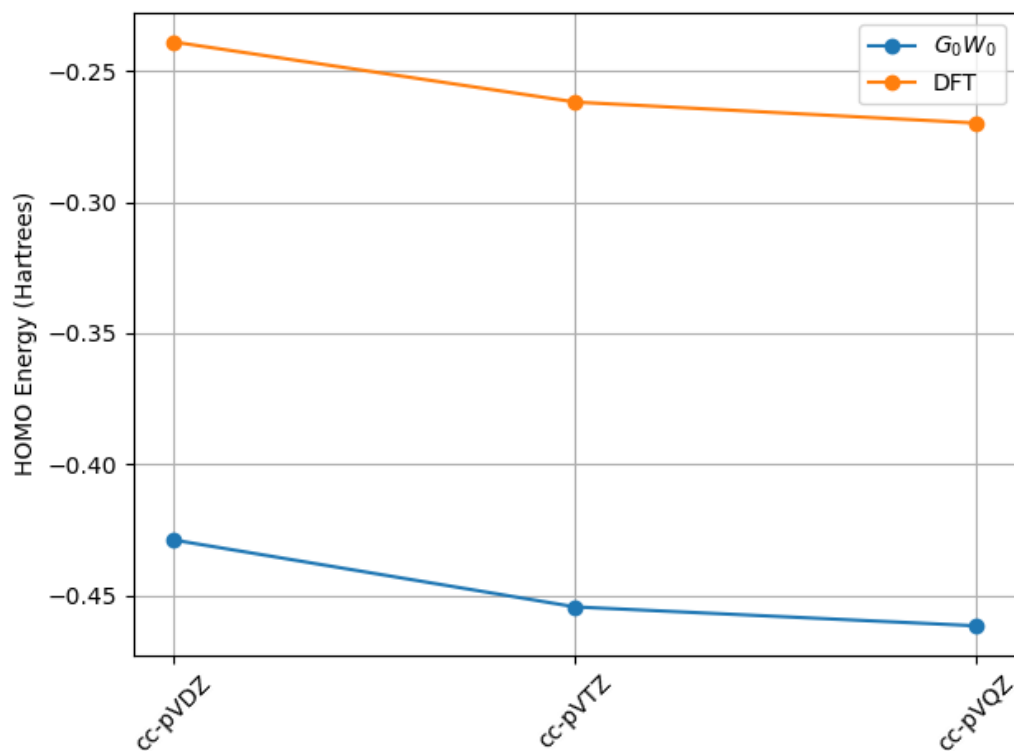


Figure 2.1: Difference in the HOMO energy for the water molecule with different bases (cc-pVDZ, etc.) for  $G_0W_0$ , and DFT, both starting from the PBE functional

## Chapter 3

### THEORETICAL BACKGROUND

We begin by writing out the Schrödinger equation for the  $N$ -electron system in a molecular field.

$$\hat{H}\Psi = E\Psi \quad (3.1)$$

with

$$\hat{H} = \sum_{i=1}^N \left( -\frac{1}{2} \nabla_i^2 \right) - \sum_{i=1}^N \sum_{\alpha} \frac{Z_{\alpha}}{r_{i\alpha}} + \sum_{i<j}^N \frac{1}{r_{ij}} \quad (3.2)$$

We note that we do not include the potential energy term associated with the nuclear-nuclear repulsion, as we are working in the Born-Oppenheimer approximation. This can be succinctly written as the sum of a kinetic energy term with a nuclear-electronic attraction term and an electron-electron repulsion term

$$\hat{H} = \hat{T} + \hat{V}_{ne} + \hat{V}_{ee} \quad (3.3)$$

The objective of many years of research in quantum chemistry has been solving for the  $V_{ee}$  term. Now, I will introduce some of the mean field methods that have been classically used to tackle this problem at a cheap computational cost.

### 3.1 Mean Field Methods

#### Hartree-Fock

In the restricted Hartree-Fock formalism, the  $V_{ee}$  is given by

$$V_{ee} = \frac{1}{2} \sum_i^{\text{occ}} \sum_j^{\text{occ}} 2(ii|jj) - (ij|ji) \quad (3.4)$$

The first term is the Coulomb term and the second term is an exchange term. We choose to make the following presentation in the restricted Hartree-Fock formalism, but considering spin here is important. In the unrestricted Hartree-Fock formalism, this would be given by

$$V_{ee} = \frac{1}{2} \sum_{\underline{i}}^{\text{occ}} \sum_{\underline{j}}^{\text{occ}} \left( (\underline{ii}|\underline{jj}) - (\underline{ij}|\underline{ji}) \right) \quad (3.5)$$

Where the underline denotes that these are spin orbitals; we have not performed the summation over all possible spins yet. The Hartree-Fock method fails to take

into account the exchange term in the unrestricted case; the integral vanishes when the spins of  $i$  and  $j$  are different. Physically, this means that there is no energetic stabilization for two electrons with different spins to occupy the same spatial index, whereas there is one when the spins are parallel. This was what was meant earlier by the statement that Hartree-Fock does not treat electron correlation.<sup>6</sup>

### Density Functional Theory (DFT)

The central quantity in DFT is the electron density, as represented by a density matrix. The method is fairly black box, and its intricate details will not be covered here (for further reading see Bruneval [8]), but it is important to understand that it treats the electron correlation through an exchange-correlation functional, which in principle has an exact form, but in practice is approximated as semi-empirical, which leads to issues in accurately describing the electron correlation from an ab-initio perspective.

What is important to understand is that both of these mean field methods yield molecular orbital energies  $\epsilon_p$  and coefficients  $C_{\mu p}$ , which we correct with MBPT methods.

### 3.2 Many-body perturbation theory

There are many different MBPT methods, but they all have the same purpose of recovering a portion of the electron correlation missed by these mean field methods. For example, Hartree-Fock is variational, meaning that its energy  $E_{HF}$  will always be greater or equal to the true energy of the system  $E_0$ . For HF, we define the difference between these two quantities as the correlation energy

$$E_{\text{corr}} \equiv E_0 - E_{HF} \quad (3.6)$$

The other mean field method that is often used is DFT, but it is not variational, so there is not such a simple interpretation of  $E_{\text{corr}}$  in this case, but the principle is similar. We will be focusing on recovering electron correlation with the  $G_0W_0$  method, which is a Green's function-based MBPT method.

## Chapter 4

### $G_0W_0$ PROCEDURE

#### 4.1 Iterative equation

The procedure that we used to compute quasiparticle energies, which are interpreted as effective molecular orbital energies, is given by

$$\delta_{pq} F_{pq}^{HF} [\gamma^{DFT}] + \Sigma^{corr}(\epsilon_p^{QP}) = \epsilon_p^{QP}. \quad (4.1)$$

We explain the notation starting from left to right. The first term corresponds to taking the diagonal of the Hartree-Fock matrix  $F_{pq}^{HF}$  evaluated at a given electron density  $\gamma$ . These electron densities are obtained from a previous mean-field calculation, either  $\gamma_{DFT}$  or  $\gamma_{HF}$ . The one-electron reduced density matrix is used to express the electron density here. The second term evaluates  $\Sigma^{corr}$  for the  $\epsilon_p^{QP}$  determined in the previous iteration. The right side of the equality gives the updated  $\epsilon_p^{QP}$ .

Equation 4.1 is iterated until self-consistency. We start with an initial guess for  $\epsilon_p^{QP}$ , which is given by the mean-field orbital energy  $\epsilon_p$ . This is used in the first iteration to solve for the right-hand side  $\epsilon_p^{QP}$  of Equation 4.1. In the next iteration, we use the previously obtained  $\epsilon_p^{QP}$  to determine  $\Sigma^{corr}$ . This process is repeated until we reach a convergence threshold for  $\epsilon_p^{QP}$ .

#### The Fock Matrix

In the basis of atomic orbitals, the HF Fock matrix is

$$F_{\mu\nu}^{HF} = h_{\mu\nu} + \sum_{\lambda\sigma} P_{\lambda\sigma} (\mu\nu|\lambda\sigma) - \frac{1}{2} \sum_{\lambda\sigma} P_{\lambda\sigma} (\mu\lambda|\nu\sigma) \quad (4.2)$$

where  $h_{\mu\nu}$  is the one-electron part of the Hamiltonian,  $P_{\lambda\sigma}$  is the one-electron reduced density matrix, and  $(\mu\nu|\lambda\sigma)$  is a two-electron integral.<sup>6</sup> A useful identity for  $P_{\lambda\sigma}$  in terms of the MO coefficients from the mean-field calculation is:

$$P_{\mu\nu} = 2 \sum_{i=1}^{N/2} C_{\mu i} C_{\nu i}^* \quad (4.3)$$

We note that the sum runs only over the  $N/2$  occupied *spatial* orbitals. Equation 4.2 is the form for the HF Fock matrix, and not the DFT Fock matrix. In the canonical

HF MO basis,  $F_{\mu\nu}^{HF}$  merely has the HF MO energies placed on the diagonal. We transform the Fock matrix into the MO basis with

$$F_{pq} = \sum_{\mu} \sum_{\nu} C_{\mu p}^* F_{\mu\nu} C_{\nu q} \quad (4.4)$$

where  $C$  is the matrix of MO coefficients.

### Correlation-Self Energy

$\Sigma^{corr}$  is the second term in Equation 4.1 and is the central quantity in the  $GW$  method. It is formed from the inputted Green's function  $G$  and the screened Coulomb potential  $W$  and recovers a portion of the  $E_{corr}$  mentioned earlier.  $\Sigma^{corr}$  is dynamic, as opposed to the previous Fock term that was discussed, as is updated with a new  $\varepsilon_p^{QP}$  in each iteration. In the case of the  $G_0W_0$  approximation, we use the common approximation, considering only the diagonal element of  $\Sigma^{corr}$  corresponding to the orbital with index  $p$ . This function is evaluated at the  $\varepsilon_p^{QP}$  just obtained in the previous iteration. To summarize, we are actually interested in  $\Sigma_{pp}^{corr}(\varepsilon_p^{QP})$ . We will go into greater detail about the form of  $\Sigma^{corr}$  in the next chapter.

### Updated $\varepsilon_p^{QP}$

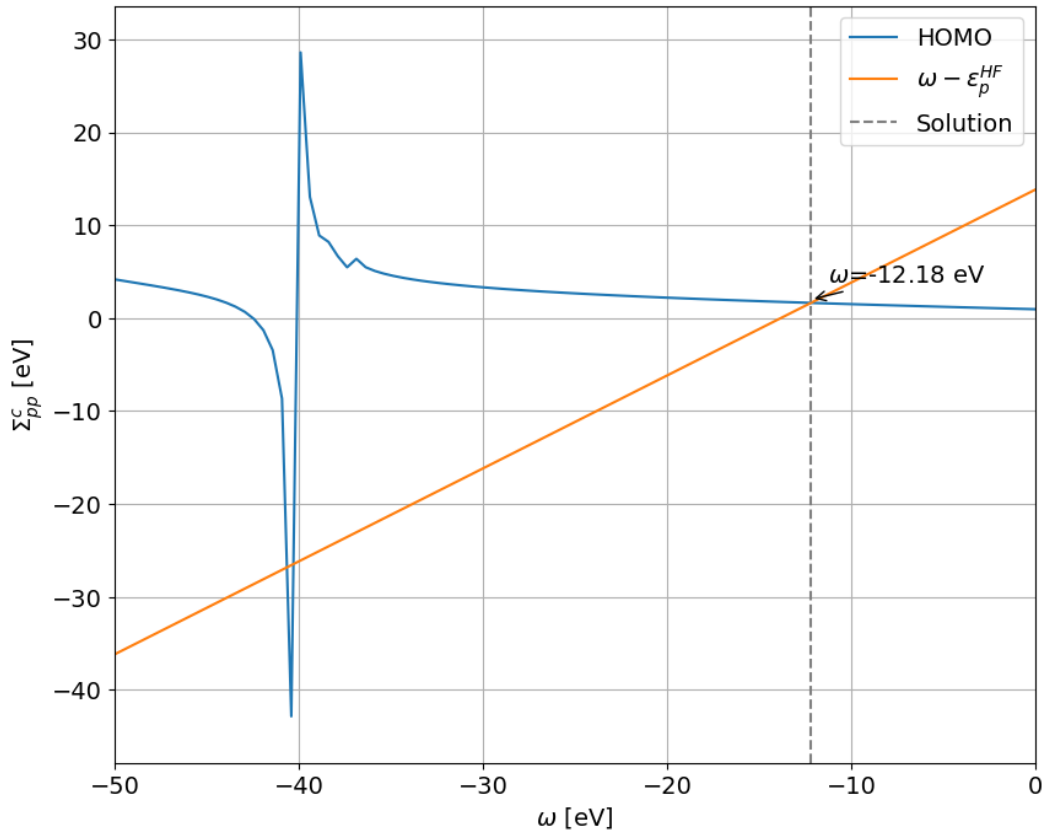
This is the right side, or the solution, of Equation 4.1.

### Graphical solution

We are able to check Equation 4.1 in the HF case by plotting  $\Sigma^{corr}$  as a function of the input frequency, which takes on the possible values for  $\varepsilon_p^{QP}$ . Since  $F_{pq}^{HF}$  is diagonal in the canonical HF MO basis, Equation 4.1 can be reformulated as

$$\epsilon_p^{HF} + \Sigma_{pp}^{corr}(\omega) = \omega \rightarrow \Sigma_{pp}^{corr}(\omega) = \omega - \epsilon_p^{HF} \quad (4.5)$$

Essentially, the line at  $\omega - \epsilon_p^{HF}$  should, and does, intersect with  $\Sigma^{corr}$  at the same  $\varepsilon_p^{QP}$  that we get from our iterative procedure, namely at the  $\omega = -12.18 \text{ eV}$ . This is a useful check to see if the self-energy, which we will derive in the next chapter, is being computed correctly.



Also, at around  $\omega = -40 \text{ eV}$ , one can observe a pole structure. This would pose problems for the convergence of my iterative procedure Equation 4.1 if the  $\varepsilon_p^{QP}$  that I was looking for was close to this  $\omega$  value, but luckily  $-12.18 \text{ eV}$  is far enough away from this pole at  $-40 \text{ eV}$ .

## 4.2 Correlation Self-Energy

$$\Sigma_{pp}^{\text{corr}}(\omega) = \sum_{\mu}^{\text{RPA}} \left( \sum_i^{\text{occupied}} \frac{\mathbf{V}_{pi}^{\mu} \mathbf{V}_{ip}^{\mu}}{\omega - (\epsilon_i - \Omega_{\mu})} + \sum_a^{\text{virtual}} \frac{\mathbf{V}_{pa}^{\mu} \mathbf{V}_{ap}^{\mu}}{\omega - (\epsilon_a + \Omega_{\mu})} \right) \quad (4.6)$$

This is the working equation for the diagonal of the correlation self-energy for a given MO. The  $\mathbf{V}^{\mu}$  and  $\Omega_{\mu}$  are the excitation vectors and energies, respectively, from a previous RPA calculation.  $\omega$  is my input frequency and the  $\epsilon$  are the orbital energies from my previous mean-field calculation.

## 4.3 Random Phase Approximation

The RPA is a linear response theory that is used to compute the excitation energies and vectors. The working matrix equation is given by<sup>7</sup>:

$$\begin{bmatrix} A & B \\ -B & -A \end{bmatrix} \begin{bmatrix} X \\ Y \end{bmatrix} = \omega \begin{bmatrix} 1 & 0 \\ 0 & -1 \end{bmatrix} \begin{bmatrix} X \\ Y \end{bmatrix} \quad (4.7)$$

where  $A$  is

$$\mathbf{A}_{ia,jb} = \delta_{ij} \delta_{ab} (\epsilon_a - \epsilon_i) + 2(ia||jb) \quad (4.8)$$

and  $B$  is

$$\mathbf{B}_{ia,jb} = 2(ia||jb) \quad (4.9)$$

The excitation vectors  $\mathbf{V}^{\mu}$  are taken by considering a contraction of two tensors. First, we consider the sum of  $\mathbf{X}$  and  $\mathbf{Y}$  at the same excitation energy  $\mu$ :  $\mathbf{Z}_{i,a,\mu} = \mathbf{X}_{i,a,\mu} + \mathbf{Y}_{i,a,\mu}$ . Then we contract this with the two-electron integrals:

$$\mathbf{W}_{p,q,i,a} = \sqrt{2} \sum_{p,q,i,a} (pq||ia) \quad (4.10)$$

This factor of  $\sqrt{2}$  comes from the spin integration of the restricted Hartree-Fock formalism. We defined a combined occupied-virtual index  $\nu$ , so:  $\mathbf{Z}_{i,a,\mu} \rightarrow \mathbf{Z}_{\nu,\mu}$  and  $\mathbf{W}_{p,q,i,a} \rightarrow \mathbf{W}_{p,q,\nu}$ .

And then we form the excitation vector from:

$$\mathbf{V}_{pq}^{\mu} = \sum_{\nu} \mathbf{W}_{p,q,\nu} \mathbf{Z}_{\nu,\mu} \quad (4.11)$$



### Tamm-Dancoff Approximation

In this method, we neglect the  $\mathbf{B}$  matrix of the RPA equation. So the eigenvalue equation becomes

$$\mathbf{A}\mathbf{X} = \omega\mathbf{X} \quad (4.12)$$

where we still have:

$$\mathbf{A}_{ia,jb} = \delta_{ij}\delta_{ab}(\varepsilon_a - \varepsilon_i) + 2(ia||jb) \quad (4.13)$$

And then we follow the same procedure as in the RPA to get  $\mathbf{V}_{pq}^\mu$ , where now we have  $\mathbf{Z}_{\nu,\mu} = \mathbf{X}_{\nu,\mu}$ .

### Direct approximation

Everywhere in the code, we consider the direct approximation, which just means that all instances of anti-symmetrized two-electron integrals are replaced by their non-symmetrized counterparts. In Equation 4.8, Equation 4.9, and Equation 4.13,  $(ia||jb) \rightarrow (ia|jb)$ . In the former case it was called the *direct* Random Phase Approximation (dRPA) and in the latter case it was called the *direct* Tamm-Dancoff Approximation (dTDA).

## Chapter 5

### LINEARIZED $G_0W_0$ DENSITY MATRIX

#### Implementation

These are the working equations for the linearized  $G_0W_0$  Density Matrix that I will derive later.<sup>8</sup> First, we consider the fully occupied block:

$$\gamma_{ij}^{GW} = 2\delta_{ij} - 2 \sum_{a\mu} \frac{\mathbf{V}_{ia}^\mu \mathbf{V}_{ja}^\mu}{(\epsilon_i - \epsilon_a - \Omega_\mu)(\epsilon_j - \epsilon_a - \Omega_\mu)} \quad (5.1)$$

where the  $\Omega_\mu$  are the excitation energies and the  $\mathbf{V}^\mu$  are the excitation vectors. The sum runs over all virtual orbitals and excitation energies. The  $\epsilon$  are the orbital energies from the prior mean-field calculation. Next, we have the virtual-virtual block:

$$\gamma_{ab}^{GW} = -2 \sum_{i\mu} \frac{\mathbf{V}_{ai}^\mu \mathbf{V}_{bi}^\mu}{(\epsilon_i - \epsilon_a - \Omega_\mu)(\epsilon_i - \epsilon_b - \Omega_\mu)} \quad (5.2)$$

Finally, we have the mixed block:

$$\gamma_{ib}^{GW} = \frac{2}{\epsilon_i - \epsilon_b} \left[ \sum_{a\mu} \frac{\mathbf{V}_{ia}^\mu \mathbf{V}_{ba}^\mu}{\epsilon_i - \epsilon_a - \Omega_\mu} - \sum_{j\mu} \frac{\mathbf{V}_{ij}^\mu \mathbf{V}_{bj}^\mu}{\epsilon_j - \epsilon_b - \Omega_\mu} \right] \quad (5.3)$$

This all contributes to the form of the density matrix as:

$$2 \begin{pmatrix} \gamma_{ij}^{GW} & \gamma_{ib}^{GW} \\ \gamma_{bi}^{GW} & \gamma_{ab}^{GW} \end{pmatrix} \quad (5.4)$$

Where  $\gamma_{bi}^{GW}$  is simply the transpose of  $\gamma_{ib}^{GW}$ , since all elements of this matrix are real. Therefore, this density matrix is Hermitian. The factor of 2 comes from the fact that we sum over both spins in the restricted Hartree-Fock formalism.

### Plotting natural occupations

The natural occupations is found by diagonalizing the density matrix. They are interpreted as being the number of electrons in a given orbital.<sup>6</sup> Here we considered the one-electron density matrix from multiple methods: We considered restricted Hartree-Fock, which contains no correlation, and Full Configuration Interaction (FCI), which contains the exact correlation. As can be seen in Figure 5.1, our implementation of the Linearized  $G_0W_0$  Density Matrix in the direct Random Phase Approximation (dRPA) and direct Tamm-Dancoff Approximation (dTDA) gives a portion of this correlation. It is interesting to see that the dTDA contains more correlation than the dRPA, as the former is a subset of the latter, and so the latter should recover more correlation. When  $H_2$  is at its equilibrium distance at a

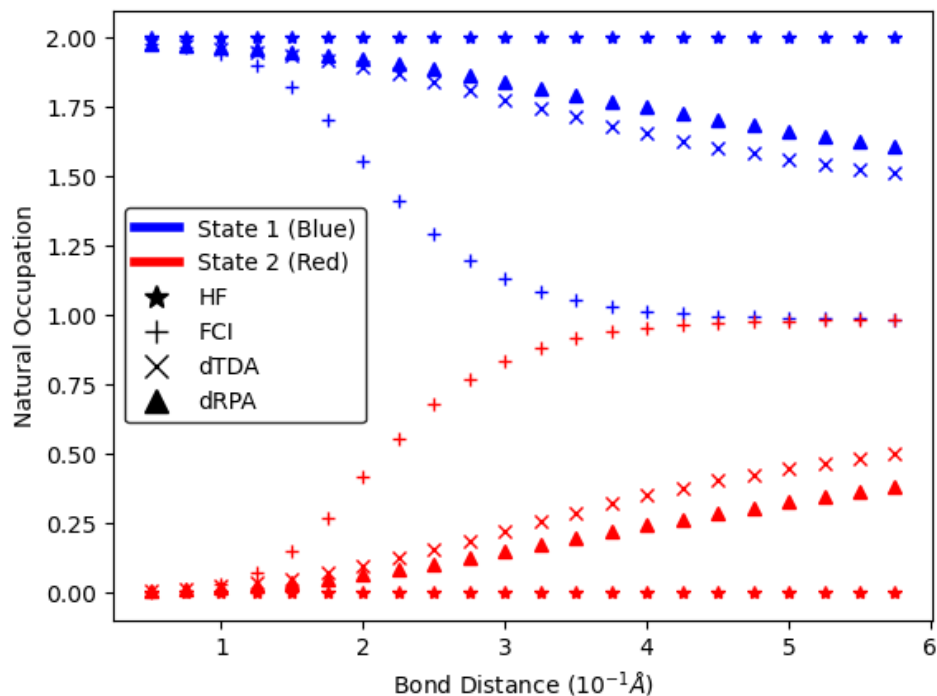


Figure 5.1: Natural occupations of the HOMO (State 1) and LUMO (State 2) of  $H_2$  along the dissociation coordinate

low bond distance, we see in Figure 5.1 that the HOMO is fully occupied with 2 electrons, while the LUMO is unoccupied. This situation is represented by the simple MO diagram in Figure 5.2. As the molecule dissociates, the occupations for the restricted Hartree-Fock method do not change at all, while FCI, containing the exact correlation, gives the expected result of the HOMO and LUMO both having

occupations of 1 electron. The dRPA and dTDA fall somewhere in between these two extremes.

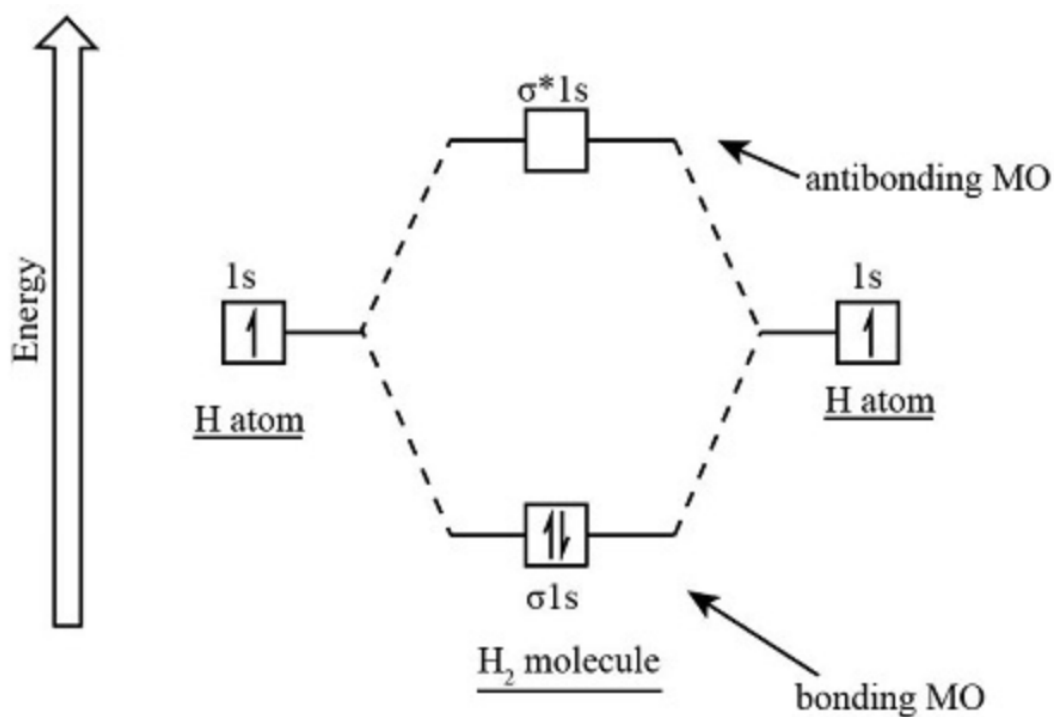


Figure 5.2: MO diagram of  $H_2$  at the equilibrium bond distance. Notice that the HOMO is fully occupied with 2 electrons, while the LUMO is unoccupied. Figure from Bruneval [8]

*Chapter 6*

THIS IS THE SIXTH CHAPTER

*Chapter 7*

THIS IS THE SEVENTH CHAPTER

*Chapter 8*

THIS IS THE EIGHTH CHAPTER

## BIBLIOGRAPHY

1. Sun, Q. *et al.* Recent developments in the PySCF program package. *The Journal of Chemical Physics* **153**, 024109. ISSN: 0021-9606. <https://doi.org/10.1063/5.0006074> (2024) (July 2020).
2. Schimka, L. *et al.* Accurate surface and adsorption energies from many-body perturbation theory. en. *Nature Materials* **9**. Publisher: Nature Publishing Group, 741–744. ISSN: 1476-4660. <https://www.nature.com/articles/nmat2806> (2024) (Sept. 2010).
3. McClain, J., Sun, Q., Chan, G. K.-L. & Berkelbach, T. C. Gaussian-Based Coupled-Cluster Theory for the Ground-State and Band Structure of Solids. *Journal of Chemical Theory and Computation* **13**. Publisher: American Chemical Society, 1209–1218. ISSN: 1549-9618. <https://doi.org/10.1021/acs.jctc.7b00049> (2024) (Mar. 2017).
4. Kozłowski, P. Elucidating Catalysis with the “Gold Standard” of Quantum Chemistry. en. *Caltech Undergraduate Research Journal*. <https://curj.caltech.edu/2021/06/29/elucidating-catalysis-with-the-gold-standard-of-quantum-chemistry/> (2024) (June 2021).
5. *Frontiers | The GW Compendium: A Practical Guide to Theoretical Photoemission Spectroscopy* <https://www.frontiersin.org/articles/10.3389/fchem.2019.00377/full> (2024).
6. Szabo, A. & Ostlund, N. S. *Modern Quantum Chemistry: Introduction to Advanced Electronic Structure Theory* en. Google-Books-ID: KQ3DAgAAQBAJ. ISBN: 978-0-486-13459-8 (Courier Corporation, June 2012).
7. Dreuw, A. & Head-Gordon, M. Single-Reference ab Initio Methods for the Calculation of Excited States of Large Molecules. *Chemical Reviews* **105**. Publisher: American Chemical Society, 4009–4037. ISSN: 0009-2665. <https://doi.org/10.1021/cr0505627> (2024) (Nov. 2005).
8. Bruneval, F. Assessment of the Linearized GW Density Matrix for Molecules. *Journal of Chemical Theory and Computation* **15**. Publisher: American Chemical Society, 4069–4078. ISSN: 1549-9618. <https://doi.org/10.1021/acs.jctc.9b00333> (2024) (July 2019).



*Appendix A*

## QUESTIONNAIRE

*Appendix B*

## CONSENT FORM



POCKET MATERIAL: MAP OF CASE STUDY SOLAR  
SYSTEMS